Simulation of Hydrodesulfurization Reactive Column Using the Research Institute of Petroleum Industry Method

ARTICLE *in* INDUSTRIAL & ENGINEERING CHEMISTRY RESEARCH · FEBRUARY 2009

Impact Factor: 2.59 · DOI: 10.1021/ie801503m

5 AUTHORS, INCLUDING:

Hamid reza Mahdipoor
Research Institute of Petroleum Industry (…
7 PUBLICATIONS **14** CITATIONS
SEE PROFILE

Keyvan Khorsand
Research Institute of Petroleum Industry (…
2 PUBLICATIONS **2** CITATIONS
SEE PROFILE

Mehdi Mohammadi
Research Institute of Petroleum Industry (…
9 PUBLICATIONS **28** CITATIONS
SEE PROFILE

Javad Alaei kadijani
Research Institute of Petroleum Industry (…
9 PUBLICATIONS **6** CITATIONS
SEE PROFILE

Simulation of Hydrodesulfurization Reactive Column Using the Research Institute of Petroleum Industry Method

Hamid Reza Mahdipoor,*,† Keyvan Khorsand,† Mehdi Mohammadi,‡ Javad Alaei,‡ and Morteza Tajerian‡

Process Engineering Department and Refinery Department, Research Institute of Petroleum Industry, West Boulevard of Azadi Stadium, P.O. Box 14665-1998, Tehran, Iran

In the new hydrodesulfurization (HDS) process by integrating the reaction and separation units in a single reactive column, the fixed cost and operational costs can be reduced, as well as more flexible operating conditions will be achievable. For investigating both the design and the operating aspects of reactive columns, computer simulation is needed. This study was performed using the RIPI (Research Institute of Petroleum Industry) method in different conditions such as various operating temperatures and pressures. For verifying the presented solving method, the results of simulating a typical *n*-butane absorber column by RIPI method were compared to the achieved results from the well-known inside-out method. The results show the capability of the RIPI method in converging the computations. Moreover, by substituting the power law model by the Langmuir−Hinshelwood kinetic model in computations, the effect of pressure variations on the HDS reactive column was investigated.

Introduction

Sulfur compounds in crude oil and cracking products, in the presence of the catalyst, react with hydrogen and convert to hydrogen sulfide and sulfur-free hydrocarbon. One of the most common processes that is used for desulfurization of oil cuts such as gas oil, kerosene, etc., is the hydrodesulfurization (HDS) process. The HDS reaction can be generally shown as[1,2]

$$R-SH + H_2 \rightarrow R-H + H_2S \quad (1)$$

In the conventional HDS units, after reaction between sulfur compounds and hydrogen in a trickle-bed reactor, the produced gas should be passed through the separators and a stripper column, to separate H_2S and remaining H_2 gases from the sweetened liquid oil. Using a reactive column is more efficient than the conventional separation/reaction schemes because it integrates the reaction and the separation in a single operating equipment. The HDS via reactive column may improve the efficiency of the conventional HDS unit because it uses the reactants, the energy, and the services efficiently. This reduces the fixed cost and operational costs.[3] Furthermore, the disadvantages of using the cocurrent gas−liquid down flow trickle-bed reactors for hydroprocessing of heavy oils is that reactions such as hydrodesulfurization and hydrogenation are inhibited by hydrogen sulfide formed.[4]

The removal of sulfur from heavy oil generally follows second-order kinetics in sulfur concentration, which is a reflection of the presence of a variety of sulfur containing compounds with different reactivities. The second-order kinetics imply that a relatively large proportion of sulfur is removed in an early stage of the process (due to conversion of the bulk of reactive molecules), while removal of the remaining sulfur takes place much more slowly in later stages. This means that the bulk of the H_2S is generated in a small inlet part of the bed and that this H_2S exerts its inhibiting influence in the remaining part of the bed. It can be seen that in cocurrent operation the larger part of the bed operates under a H_2S-rich regime. The situation is clearly more favorable in the counter-current mode of operation because in this case the major part of the bed operates in the H_2S lean regime.[5] The counter-current reactor shown in Figure 1 is essentially a reactive column wherein the H_2S is stripped from the liquid phase and carried to the top. Other examples of application of reactive distillation can be found in esterification processes,[3,6] separation of isomers,[7] and in the manufactures of "antiknock" enhancers such as methyl *tert*-butyl ether (MTBE) and *tert*-amyl methyl ether (TAME).[8,9]

There are a wide range of sulfur compounds in an oil cut, the type of which depends on the boiling range of the cut. When the oil cut is heavier, its sulfur compounds will be heavier and more difficult to remove. In this work, the dibenzothiophene (DBT) is used to represent the sulfur compounds because it is one of the less reactive sulfur organic compounds present in gas oil. In addition, its concentration is significant. For kinetic modeling of a chemical reaction, several models such as power law, Langmuir−Hinshelwood, and Riedel can be used. In this study, the first two models were applied in the simulations. The related equations of these models are presented in the next section.[10]

Modeling of reactive separation processes requires simultaneous prediction of reaction and separation. Several alternatives

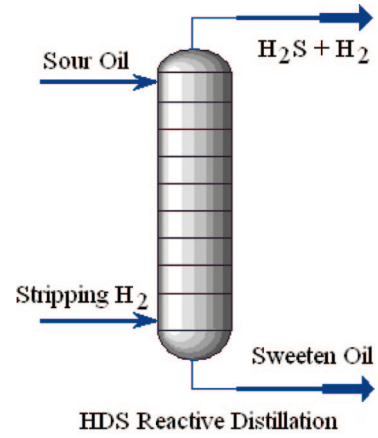

Figure 1. Schematic shape of the HDS reactive stripper column.

* Corresponding author. E-mail: mahdipoorhr@ripi.ir.
† Process Engineering Department.
‡ Refinery Department.

10.1021/ie801503m CCC: $40.75
Published on Web 01/05/2009

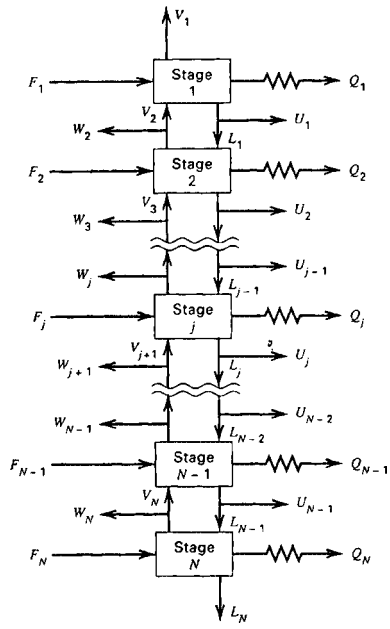

Figure 2. General form of N consecutive counter-current stages.

are possible. For example, treat the process as a nonequilibrium system (kinetically controlled reaction plus separation through mass/heat transfer), treat the process as only in physical equilibrium with the kinetically controlled reaction, or treat the process as an equilibrium process (chemical and physical equilibrium).[11] The RIPI method was presented to solve the equilibrium-based equations of distillation column models. Using a tray by tray algorithm and the shooting method, RIPI method has a high flexibility for implementing the heating and cooling in the column stages and using the kinetic equations in the form of the Langmuir−Hinshelwood equation or the power law kinetic equation.

For verifying the presented algorithm, the results of simulating a typical n-butane absorber column were compared to the achieved results from a commercial simulator. The results show the capability of the RIPI method in converging the computations. Furthermore, the effect of pressure variations on the HDS reactive column was investigated by applying the Langmuir−Hinshelwood kinetic model.

Mathematical Modeling and Kinetic Characteristics

With respect to Figure 2, the basic equations usually used in steady-state distillation column modeling (MESH equations) are shown below.[12]

Mass balance:

$$M_{i,j} = L_{j-1}x_{i,j-1} + V_{j+1}y_{i,j+1} + F_j z_{i,j} - (L_j + U_j)x_{i,j} - (V_j + W_j)y_{i,j} + V_{H_j}\sum_{n=1}^{NR} \nu_{i,n} r_{j,n} = 0 \quad (2)$$

Equilibrium:

$$E_{i,j} = y_{i,j} - k_{i,j}x_{i,j} = 0 \quad (3)$$

Summation:

$$(Sy)_i = \sum_{i=1}^{C} y_{i,j} - 1.0 = 0 \quad (4)$$

$$(Sx)_i = \sum_{i=1}^{C} x_{i,j} - 1.0 = 0 \quad (5)$$

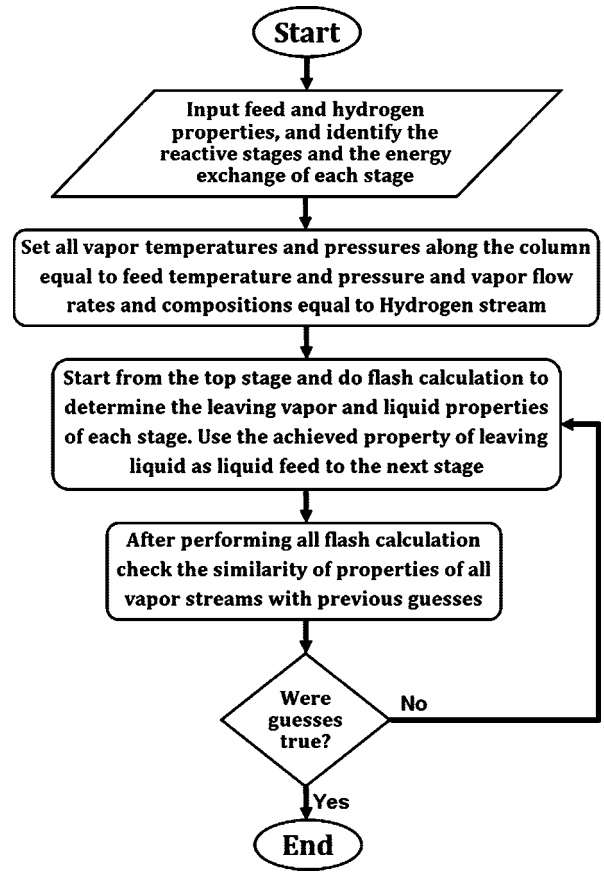

Figure 3. The RIPI method algorithm.

Energy balance:

$$H_j = L_{j-1}h_{L_{j-1}} + V_{j+1}h_{V_{j+1}} + F_j h_{F_j} - (L_j + U_j)h_{L_j} - (V_j + W_j)h_{v_j} - Q_j + Q_r = 0 \quad (6)$$

The new algorithm developed at RIPI is shown in Figure 3. In contrast with the conventional methods such as simultaneous correction or homotopy continuation, the RIPI method, after assuming a series of initial assumptions such as liquid and vapor flows, and temperature and concentration profiles along the column, solves stage by stage the MESH equations (i.e., performing the flash calculations). The initial values can then be modified by replacing the new obtained values. This modification can be carried out in different ways. For instance, after performing the flash calculation for stage j, the obtained specs for stream L_j, which leaves stage j as liquid product, are used as the specs of liquid feed for stage $j + 1$ (i.e., L_{j+1}). This will be continued until the flash calculations for all stages are finished. At the end of each computational step, the error of computations can be estimated by the following equation:

$$\varepsilon = \sum_{j=2}^{NS}\left((T_j^{VP} - T_{j-1}^{VF})^2 + (F_j^{VP} - F_{j-1}^{VF})^2 + \sum_{i=1}^{NC}(y_{i,j}^{VP} - y_{i,j-1}^{VF})^2\right)^{0.5} \quad (7)$$

VP and VF in eq 7 refer to specs of vapor product and vapor feed, respectively. Because the vapor product of each stage is equal to the vapor feed of its upper stage (the properties of this stream are assumed or calculated at the previous step), the convergence is achieved when all of their specs were the same.

Moreover, F_0, $z_{i,0}$, and $h_{F,0}$ in the mentioned equations are the flow rate, concentration, and enthalpy of the liquid feed stream entered into tray 1, respectively. In addition, F_N, $z_{N,0}$,

and $h_{N,0}$ are the flow rate, concentration, and enthalpy of the vapor feed stream entered from the bottom of the column. Because the reactive column in the present work is assumed to be a reactive absorber, the flow rates of other feed streams were set equal to zero.

The reaction of dibenzothiophene (DBT) and hydrogen (H_2) can be simply shown as below:

$$\mathrm{DBT} + 2\mathrm{H_2} \rightarrow \mathrm{BiPh} + \mathrm{H_2S} \tag{8}$$

where BiPh is biphenyl. Shokri et al.[13] proposed the following power law kinetic model for this reaction:

$$r_{\mathrm{DBT}} = \frac{\mathrm{d}C_{\mathrm{DBT}}}{\mathrm{d}t} = -kC_{\mathrm{DBT}}^{n} \tag{9}$$

If the reaction order was zero or greater than 1, the solving of eq 9 will result as below:

$$\frac{1}{n-1}\left[\frac{1}{C_{\mathrm{p}}^{n-1}} - \frac{1}{C_{\mathrm{f}}^{n-1}}\right] = \frac{k}{\mathrm{LHSV}} \tag{10}$$

where C_{p} and C_{f} are reactant concentration in product and feed streams based on weight percent, respectively. n is the reaction order, and LHSV is the heterogeneous catalytic reactions parameter (h^{-1}), which is equal to the ratio of catalyst volume to feed volumetric flow rate. Also, k is the reaction constant, which is defined as below:

$$k = k_0 \exp\left(-\frac{E}{RT}\right) \tag{11}$$

where k_0 is the Arrhenius constant, E is the reaction activation energy (kJ/kmol), R is the gas constant (kJ/mol·K), and T is the temperature (K). According to the experiments accomplished by Shokri et al.,[13] the HDS reaction order (n) for gas oil feed is equal to 1.5, and k_0 and E are 2.7×10^9 and 92 660 kJ/kmol, respectively. Also, with respect to feed flow rate in the simulations (i.e., 1 L/h) and selecting a catalyst volume of 1 L, LHSV become equal to 1 h^{-1}, which is an appropriate value in practice. Therefore, if 20 equilibrium reactive stages be considered, the catalyst volume for each stage will be equal to 1/20 L. Therefore, in this manner, it is supposed that each stage operate as a CSTR reactor with the volume of 1/20 L, and the liquid and vapor phases are completely mixed.

Moreover, using the kinetics proposed by Broderick and Gates[14] in the form of the Langmuir−Hinshelwood equation, it is possible to consider the effect of pressure changes and H_2S and H_2 concentrations in the simulation calculations. In this case, DBT reacts via two parallel pathways, the hydrogenolysis that was shown in eq 8, and the hydrogenation:

$$\mathrm{DBT} + 5\mathrm{H_2} \rightarrow \mathrm{CHB} + \mathrm{H_2S} \tag{12}$$

where CHB is cyclohexylbenzene. The reaction rate equations of the hydrogenolysis and hydrogenation are presented in eqs 12 and 13, respectively.

$$r_{\mathrm{hs}} = \frac{kK_{\mathrm{DBT}}K_{\mathrm{H_2}}C_{\mathrm{DBT}}C_{\mathrm{H_2}}}{(1 + K_{\mathrm{DBT}}C_{\mathrm{DBT}} + K_{\mathrm{H_2S}}C_{\mathrm{H_2S}})^2(1 + K_{\mathrm{H_2}}C_{\mathrm{H_2}})} \tag{13}$$

$$r_{\mathrm{hn}} = \frac{k'K'_{\mathrm{DBT}}K'_{\mathrm{H_2}}C_{\mathrm{DBT}}C_{\mathrm{H_2}}}{1 + K'_{\mathrm{DBT}}C_{\mathrm{DBT}}} \tag{14}$$

wherein the kinetic coefficients are defined as below:

$$k = k_{\mathrm{a_1}} e^{(k_{\mathrm{a_2}}/RT)} \tag{15}$$

$$K_{\mathrm{DBT}} = k_{\mathrm{a_3}} e^{(k_{\mathrm{a_4}}/RT)} \tag{16}$$

$$K_{\mathrm{H_2}} = k_{\mathrm{a_5}} e^{(k_{\mathrm{a_6}}/RT)} \tag{17}$$

$$K_{\mathrm{H_2S}} = k_{\mathrm{a_7}} e^{(k_{\mathrm{a_8}}/RT)} \tag{18}$$

$$k'K'_{\mathrm{H_2}} = k_{\mathrm{b_1}} e^{(k_{\mathrm{b_2}}/RT)} \tag{19}$$

$$K'_{\mathrm{DBT}} = k_{\mathrm{b_3}} e^{(k_{\mathrm{b_4}}/RT)} \tag{20}$$

The values of k_{a_i} and k_{b_i} are presented in Table 1.

Method Confirmation

Because the simulation of the HDS reactive column with available commercial simulator in different operating conditions was not possible, for investigating the performance of the presented method, the results of simulation of *n*-butane column using RIPI method were compared to achieved results by the inside-out method, which is a common method in commercial simulators. This column was equipped with 10 equilibrium stages and used for separating *n*-butane from a C1 to C5 gas solution by using *n*-C15 as absorbent. The characteristics of absorbent oil entering from the top of the column, and gas solution entering from the bottom of the column, are presented in Tables 2 and 3, respectively.

The changes of temperature, molar flow of liquid, and molar flow of vapor along the absorber column are presented in Figures 4, 5, and 6, respectively. As illustrated in these figures, the results obtained from the RIPI method agree with the results of the inside-out method. In addition to the above simulation, the capability of the RIPI method was verified by simulation of the reactive H_2S absorber column in the amine gas sweetening unit, which yielded appropriate results too.

Simulation of HDS Reactive Column

In this section, a reactive column with 20 theoretical stages is simulated. The characteristics of the gas oil feed entered from

Table 1. Kinetic Constants for Hydrogenolysis and Hydrogenation[14]

coefficient	unit	value
$k_{\mathrm{a_1}}$	(mol/(gCAT·s))	787 000
$k_{\mathrm{a_2}}$	(cal/mol)	−30 115
$k_{\mathrm{a_3}}$	(L/mol)	0.18
$k_{\mathrm{a_4}}$	(cal/mol)	4541
$k_{\mathrm{a_5}}$	(L/mol)	4000
$k_{\mathrm{a_6}}$	(cal/mol)	−8365
$k_{\mathrm{a_7}}$	(L/mol)	0.7
$k_{\mathrm{a_8}}$	(cal/mol)	5258
$k_{\mathrm{b_1}}$	(L/(gCAT·s))	42 194
$k_{\mathrm{b_2}}$	(cal/mol)	−27 728
$k_{\mathrm{b_3}}$	(L/mol)	1.999
$k_{\mathrm{b_4}}$	(cal/mol)	1433.8

Table 2. Characteristics of Absorbent Entered into the Absorber Column

property	value
molar flow	55 kmol/h
temperature	30 °C
pressure	27 bar

Table 3. Characteristics of Gas Solution Entered into the Absorber Column

property	value
molar flow	360 kmol/h
temperature	40 °C
pressure	27 bar
C1 (wt %)	0.100
C2 (wt %)	0.420
C3 (wt %)	0.410
C4 (wt %)	0.055
C5 (wt %)	0.015

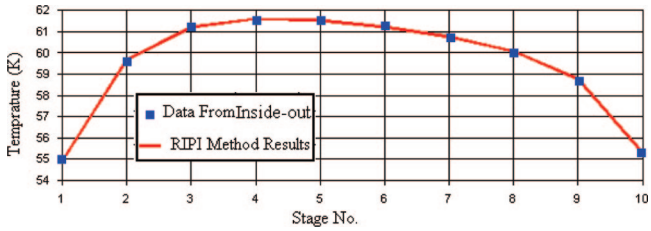

Figure 4. The changes of temperature along the absorber column in simulation with inside-out and RIPI methods.

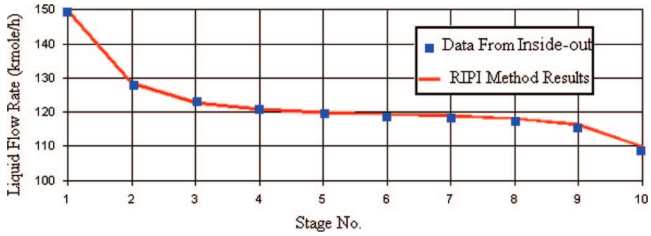

Figure 5. The changes of molar flow of liquid along the absorber column in simulation with inside-out and RIPI methods.

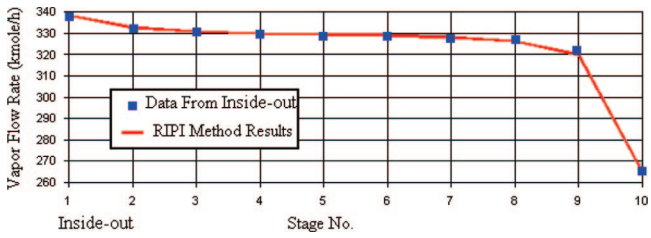

Figure 6. The changes of molar flow of vapor along the absorber column in simulation with inside-out and RIPI methods.

Table 4. Characteristics of the Gas Oil Feed Entered into the HDS Reactive Column

property	value
volume flow	1 L/h
temperature	370 °C
pressure	70 bar
mass fraction of DBT	0.0691

Table 5. Characteristics of the Hydrogen Gas Entered into the HDS Reactive Column

property	value
mass flow	0.0222 kg/h
temperature	370 °C
pressure	70 bar

the top of the column and the hydrogen stream entered from the bottom of the column are presented in Tables 4 and 5, respectively. Regarding the mass fraction of DBT presented in Table 4, the ppm of sulfur in the gas oil feed can be easily computed from the molecular weight of DBT, which will be equal to 12 000.

Figure 7 shows the temperature profile along the reactive column. As indicated in this figure, the temperature of stages 1−16 was almost constant and equal to 370 °C. Because the solving of hydrogen in the gas oil is endothermic, the temperature decreased after stage 8.

Figures 8 and 9 present the changes in mass flow rates of liquid and gas, respectively. According to Figure 8, there is a decreasing path for mass flow rates of liquid. Figure 9 shows the same trend for mass flow rates of gas along the column. At first, it can be guessed that the decreasing path is because of converting the liquid-phase dibenzothiophene (DBT) to gas-

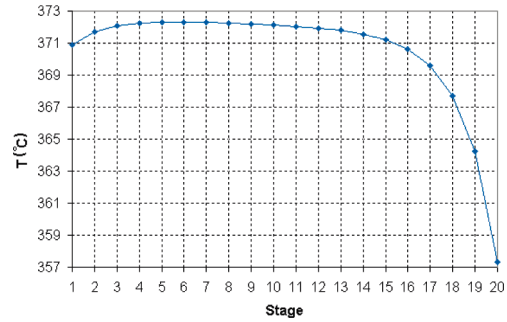

Figure 7. The temperature profile along the HDS reactive column.

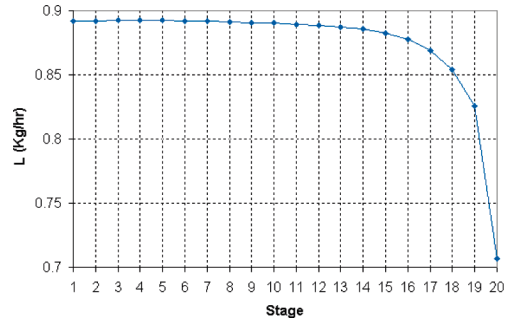

Figure 8. The changes in mass flow rates of liquid stream along the HDS reactive column.

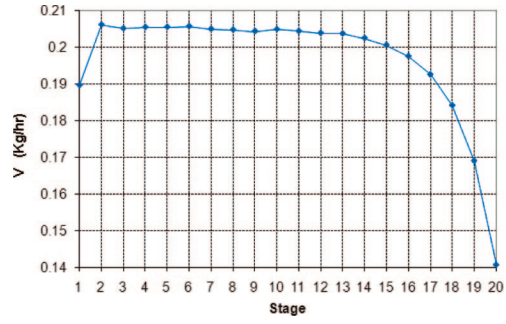

Figure 9. The changes in mass flow rates of gas stream along the HDS reactive column.

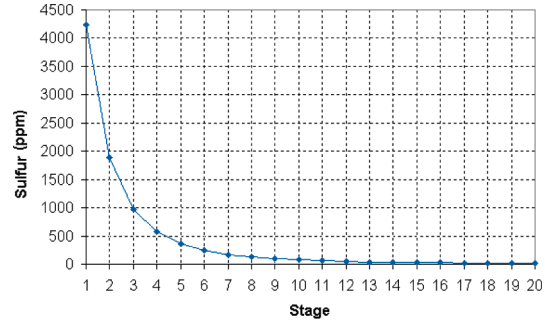

Figure 10. The sulfur content of liquid stream along the HDS reactive column.

state H_2S. Yet, as will be illustrated in Figure 10, most of the DBT will react at the earlier stages, and the reaction does not have a significant effect on the flow rates in the final stages. By exact investigating the changes of all vapor components along the column, it was observed that by increasing the temperature at the stages before stage 19 (see Figure 7), some of the lighter components in the gas oil liquid stream were vaporized and carried by H_2 gas toward the upper stages. Because the reaction of DBT and hydrogen is exothermic, the

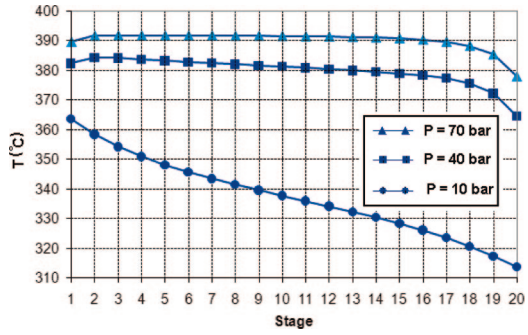

Figure 11. Temperature changes along the HDS reactive column in the case of using Langmuir−Hinshelwood equations.

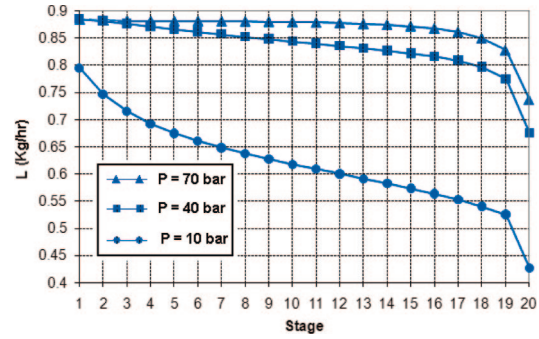

Figure 12. The variations of liquid mass flow rate along the HDS reactive column in the case of using Langmuir−Hinshelwood equations.

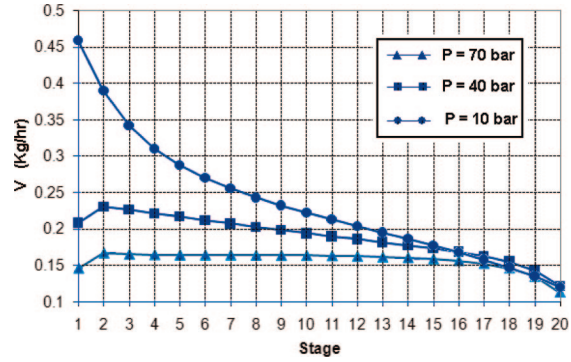

Figure 13. The variations of vapor mass flow rate along the HDS reactive column in the case of using Langmuir−Hinshelwood equations.

gas oil that entered at 370 °C becomes a bit warmer after the beginning stages. Therefore, the temperature of the gas stream when it reaches to top of the column and contacts with fresh feed will decrease, and some of the light component in the gas stream will be liquefied. This can explain the reason for the sudden decline in vapor flow at stage 1.

Figure 10 shows the sulfur content of liquid stream along the column. As is shown in this figure, the sulfur content has reached its proper range, that is, under 50 ppm, next to stage 10. The sulfur content of stage 1 in the horizontal axis shows the value of sulfur content related to the exit of stage 1; that is, in the first stage the content of sulfur is decreased from 12 000 to about 4200 ppm. According to this figure, the existence of just 10 stages seems to be enough to obtain the acceptable range of the sulfur content, but because the entered hydrogen decreases the column temperature, the other stages may be necessary to keep the stages temperature near the appropriate reaction temperature. However, one of the outcomes of this study can be determining the required equilibrium and reactive stages.

To investigate the effect of the pressure changes on the HDS reactive column, using Langmuir−Hinshelwood equations (eqs 13 and 14), three simulations at 10, 40, and 70 bar pressures were performed. Other conditions such as temperature, feed and hydrogen flow rates, and the concentration of DBT in the feed stream were similar to data presented in Tables 4 and 5.

Figure 11 shows the temperature profile along the reactive column in the case of using Langmuir−Hinshelwood equations in the above-mentioned pressures. As it can be seen in this figure, when the column pressure is equal to 70 bar, the temperature increases to 390 °C. The reason for the increase in the temperature profile can be explained by a large amount of heat-released exothermic reactions. Also, a decrease in the temperature of the last stages can be described by endothermic mixing of the hydrogen entered from the bottom of the column with the downward gas oil stream. In comparison with previous simulations performed using the power law kinetic equation, as described before, the present simulations that apply the Langmuir−Hinshelwood kinetic equation consist of two exothermic reactions, while the power law equation only uses one reaction, that is, hydrogenolysis. Therefore, the predicted temperature in the case of using the Langmuir−Hinshelwood equation was higher than the manner of applying the power law equation.

Temperature along the reactive column in the case of using Langmuir−Hinshelwood equations at 70 bar pressure possesses greater values in comparison with the simulations performed at pressures equal to 40 and 10 bar. This is because of the occurrence of less reaction at lower pressures. The temperature along the column at 10 bar pressure has considerably lower values in comparison with the two other pressures, while temperature changes at 40 and 70 bar do not have important differences.

Figures 12 and 13 show mass flow rates of liquid and vapor streams along the HDS reactive column in the case of using Langmuir−Hinshelwood equations at pressures of 10, 40, and 70 bar. By comparing the achieved mass flow rates of liquid and vapor streams at these pressures, it can be found that there is not a considerable difference between the obtained results for 70 and 40 bar pressures, but the liquid mass flow rate along the column at 10 bar pressure has considerably lower values. It can be explained by the same reason as that described before in a previous simulation. Because the column operates at lower pressure, therefore, the vaporization will be more than that when operating at 70 and 40 bar pressures. This can be obviously observed in Figure 13, which shows the variations of vapor flow rate along the column. Vapor flow at the upper stages for operating at 40 bar pressure is more than the case of operating at 70 bar pressure, and vapor flow at 40 bar is more than that operating at 70 bar too.

Moreover, the changes of sulfur content in the liquid stream along the reactive column in the case of using Langmuir−Hinshelwood equations have been presented in Figure 14. By attending to this figure, it seems that the sulfur content at 10 bar pressure is reduced similar to other two pressures, and the result is satisfactory. Yet, by more consideration to achieved simulation results, it can be found that when the pressure of the column is 10 bar, more than 60 mass percent of DBT is vaporized and leaves the column together with the upward gas stream. This loss at 40 and 70 bar pressure is 10 and 4 wt %, respectively. Therefore, it can be deduced that operating at 10 bar pressure would not be proper for the hydrodesulfurization reactive distillation process.

Despite some disadvantages of the algorithm such as the long computation times or the larger residue convergence error as

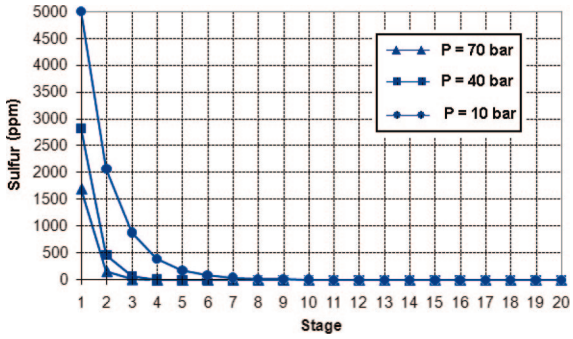

Figure 14. The sulfur content of liquid stream along the HDS reactive column in the case of using Langmuir−Hinshelwood equations.

compared to common algorithms, this method can be useful when the other methods are not able to converge or achieve results. For instance, some simulations were performed when the feed was entered at ambient temperature, that is, 25 °C, and some of the column staged was heated (e.g., entering 40 W to each stage) to constant temperature along the column (the reaction temperature). This condition is similar to the pilot scale reactive columns, which can be heated by external electrical jackets. The achieved results show the converging capability of the RIPI method under different heating conditions, while some of the commercial simulators could not converge toward the results, and some others were very sensitive in terms of the heating conditions.

Furthermore, some other simulations were performed when more than one hydrogen stream entered into the column from the middle stages. These hydrogen streams act as the quenching agent and are used for controlling the temperature profile along the HDS reactive columns. Although this algorithm was used to simulate an absorber reactive column, by more computer programming, it can be generally used for the simulation of the other distillation column types. Moreover, with applying the kinetic models in the form of the Langmuir−Hinshelwood equation, analyzing the effect of pressure changes on the reactive column behaviors would be possible, while it is not easily achievable in the commercial simulators.

Because the concept of using reactive columns instead of reactor and stripper column is a new idea and still under development, the presented results can be useful to better design or operate the HDS reactive columns. Conversely, the achieved results from a pilot plant reactive column can help to improve the simulator and adjust its parameters for future uses.

Conclusions

In a new hydrodesulfurization (HDS) process, by replacing a reactive column instead of separators and stripper, fixed and working capital can be reduced, and also it is possible to work in modified operating conditions such as lower temperature and/or lower pressure. In this work, using a new method developed at the Research Institute of Petroleum Industry (RIPI), a computer simulation was performed to evaluate the design and operation aspects of a HDS reactive column for gas oil feedstock. This method was able to use the kinetic models in the form of the Langmuir−Hinshelwood equation and, therefore, investigate the effect of pressure changes on the reactive column behaviors. Moreover, the performance of the presented method was verified by achieving the proper results in simulating the absorber columns, as well as by solving and converging the reactive model equations.

Acknowledgment

We are grateful to the Research Institute of Petroleum Industry (RIPI) for supporting this work.

Nomenclature

C = concentration
E = activation energy
F = feed flow rate
H = enthalpy
h = specific enthalpy
K = adsorption constant for the hydrogenolysis reaction
K' = adsorption constant for the hydrogenation reaction
k = reaction rate constant
k_o = Arrhenius constant
L = liquid flow rate
m = mass
NC = number of components
NR = number of reactions
NS = number of stages
P = pressure
Q = heat flow rate
R = gas constant
r = reaction rate
S = summation
T = temperature
U = liquid side stream flow rate
V = vapor flow rate
wt = weight
V_H = volumetric liquid holdup
W = vapor side stream flow rate
x = liquid component fraction
y = vapor component fraction
z = feed component fraction

Superscripts

n = reaction order
VF = vapor feed
VP = vapor product

Subscripts

r = reaction
i = component index
j = stage index
p = product
f = feed
n = reaction order

Greek Symbols

ν = stoichiometric coefficient

Abbreviations

BiPh = biphenyl
CHB = cyclohexylbenzene
DBT = dibenzothiophene
LHSV = liquid hourly space velocity

Literature Cited

(1) Diaz-Real, R. A.; Mann, R. S.; Sambi, I. S. Hydrotreatment of athabasca bitumen derived gas oil over nickel−molybdenum, nickel−tungsten, and cobalt−molybdenum catalysts. *Ind. Eng. Chem. Res.* **1993**, *32*, 1354.

(2) Bej, S. K.; Dalai, A. K.; Adjaye, J. Comparison of hydrodenitrogenation of basic and non-basic nitrogen compounds present in oil sands derived heavy gas oil. *Energy Fuels* **2001**, *15*, 377.

(3) Agreda, V. H.; Partin, L. R.; Heise, W. H. High purity methyl acetate via reactive distillation. *Chem. Eng. Prog.* **1990**, *86*, 2–40.

(4) Krishna, R.; Sie, S. T. Strategies for multiphase reactor selection. *Chem. Eng. Sci.* **1994**, *49*, 4029–4065.

(5) Taylor, R.; Krishna, R. Modeling reactive distillation. *Chem. Eng. Sci.* **2000**, *55*, 5183–5229.

(6) Sawistowski, H.; Pilavachi, P. A. Performance of esterification in a reaction-distillation column. *Chem. Eng. Sci.* **1988**, *43*, 355.

(7) Saito, S.; Michishta, T.; Maeda, S. Separation of *meta*- and *para*-xylene mixture by distillation accompanied by chemical reactions. *J. Chem. Eng. Jpn.* **1971**, *4*, 37.

(8) Giessler, S.; Danilov, R. Y.; Pisarenko, R. Y.; Seramov, L. A.; Hasebe, S.; Hashimoto, I. Feasibility study of reactive distillation using the analysis of statics. *Ind. Eng. Chem. Res.* **1998**, *37*, 2220–2225.

(9) Bravo, J. L.; Pyhalathi, A.; Jaervelin, H. Investigations in a catalytic distillation pilot plant: Vapor/liquid equilibrium, kinetics and mass transfer issues. *Ind. Eng. Chem. Res.* **1993**, *32*, 2220–2225.

(10) Mohammadi, M.; Tajerian, M.; Shokri, S.; Dehghani, A.; Mahdipoor, H. R. Kinetics of HDS Reaction for South Pars Gas Condensate. *Iranian J. Chem. Chem. Eng.* **2008**, *48*, 93–102.

(11) Vargas-Villamil, F. D.; Marroquin, J. O.; de la Paz, C.; Rodriguez, E. A catalytic distillation process for light gas oil hydrodesulfurization. *Chem. Eng. Process.* **2004**, 43.

(12) Seader, J. D.; Henley, E. J. *Separation Process Principles*; John Wiley & Sons: New York, 1997.

(13) (a) Shokri, S.; Tajerian, M.; Mohammadi, M.; Dehghani, A.; Ganji, H.; Javaherizadeh, H. Kinetic of gas oil HDS reaction *Sharif*, in press, 2008. (b) Shokri, S.; Tajerian, M.; Mohammadi, M.; Seifmohadesi, R. Determining of a kinetic model for the hydrodesulfurization reaction of dibenzothiophene in petroleum cuts. Presented at the 11th Iranian Congress of Chemical Engineering, Tehran, Iran, 2006.

(14) Broderick, D. H.; Gates, B. C. Hydrogenolysis and hydrogenation of dibenzothiophene catalyzed by sulfided CoO-MoO_3/Al_2O_3: the reaction kinetics. *AIChE J.* **1981**, *27*, 4.

Received for review July 29, 2008
Accepted November 4, 2008

IE801503M